scientific reports

Check for updates

OPEN

Different electrostatic forces drive the binding kinetics of SARS-CoV, SARS-CoV-2 and MERS-CoV Envelope proteins with the PDZ2 domain of ZO1

Valeria Pennacchietti & Angelo Toto ✉

The Envelope protein (E) is a structural protein encoded by the genome of SARS-CoV, SARS-CoV-2 and MERS-CoV Coronaviruses. It is poorly present in the virus but highly expressed in the host cell, with prominent role in virus assembly and virulence. The E protein possesses a PDZ-binding motif (PBM) at its C terminus that allows it to interact with host PDZ domain containing proteins. ZO1 is a key protein in assembling the cytoplasmic plaque of epithelial and endothelial Tight Junctions (TJs) as well as in determining cell differentiation, proliferation and polarity. The PDZ2 domain of ZO1 is known to interact with the Coronaviruses Envelope proteins, however the molecular details of such interaction have not been established. In this paper we directly measured, through Fluorescence Resonance Energy Transfer and Stopped-Flow methodology, the binding kinetics of the PDZ2 domain of ZO1 with peptides mimicking the C-terminal portion of the Envelope protein from SARS-CoV, SARS-CoV-2 and MERS-CoV in different ionic strength conditions. Interestingly, the peptide mimicking the E protein from MERS-CoV display much higher microscopic association rate constant with PDZ2 compared to SARS-CoV and SARS-CoV-2 suggesting a stronger contribution of electrostatic forces in the early events of binding. A comparison of thermodynamic and kinetic data obtained at increasing ionic strengths put in evidence different contribution of electrostatics in the recognition and complex formation events for the three peptides. Our data are discussed under the light of available structural data of PDZ2 domain of ZO1 and of previous works about these protein systems.

It is a common strategy among pathogens, such as viruses and bacteria, to evolve to display in their proteins consensus sequences that allows them to interact with host proteins[1], mimicking Short Linear Motifs (SLiMs) that can be recognized and bound by specific protein–protein interactions modules[2]. These interactions, which are at the basis of the regulation of almost all physiological and molecular pathways in the cell, can be disrupted by pathogens eventually leading to the development of diseases[1].

Coronaviruses (CoV) are enveloped viruses that can infect humans at level of the respiratory system, ranging from infections of the upper respiratory tract, resembling the common cold, to the lower respiratory tract causing bronchitis and pneumonia. The single stranded positive sense RNA genome of about 30 kb of Coronaviruses encodes for a series of non-structural proteins and four major structural proteins, namely the Nucleocapsid protein (N), the Membrane protein (M), the Spike protein (S) and the Envelope protein (E). The E protein is the shortest and most enigmatic of the four structural proteins. It is an integral membrane protein in which three domains can be identified: a hydrophobic transmembrane domain (TMD), responsible of the formation of an alpha-helical structure that undergoes oligomerization and subsequent constitution of an ion channel in the membrane, flanked by a short hydrophilic N-terminal domain (NTD) and the largest hydrophilic C-terminal domain (CTD)[3].

The CTD of E proteins of SARS-CoV, SARS-CoV-2 and MERS-CoV (three members of the Coronaviruses family) has been established to display, at its C terminus, a PDZ-binding motif (PBM), that is a consensus sequence recognized and bound by PDZ domains[4,5]. PDZ domains are the most abundant protein–protein

Dipartimento di Scienze Biochimiche "A. Rossi Fanelli", Laboratory Affiliated to Istituto Pasteur Italia-Fondazione Cenci Bolognetti, Sapienza Università di Roma, P.le Aldo Moro 5, 00185 Rome, Italy. ✉email: angelo.toto@uniroma1.it

interaction modules in the human proteome, representing a common target of viral pathogens, from adenoviruses, rabies, HPV to influenza[6,7]. The ability of E protein to interact with PDZ domain containing proteins is well established and it has been reported as a key event in the virulence mechanisms of the viruses, as well as in virion trafficking, assembling and budding[8]. Interestingly, engineered viruses lacking the C-terminal PBM in the E protein resulted to be less virulent in in vivo experiments, with the tendency to acquire alternative PBMs after several cell passages, confirming the importance of PDZ-mediated interactions[9,10].

One of the cellular targets of the PBM of the E protein is ZO1[11]. ZO1 is a PDZ containing protein with a critical role in assembling the cytoplasmic plaque of epithelial and endothelial Tight Junctions (TJs) as well as in determining cell differentiation, proliferation and polarity[12,13]. ZO1 exerts its scaffolding functions through its three PDZ domains and the SH3 domain, that mediate protein–protein interactions and govern the spatial arrangement of the cytosolic protein complex of TJs[12,14–16]. Interestingly, the interaction between the PDZ2 domain of ZO1 and the E protein has been suggested to be fundamental in disrupting the delicate and sophisticated mechanism of TJs assembling, possibly determining the characteristic epithelial lung damages and pulmonary disfunction that may occur upon and after CoVs infections[17–20].

Although the interaction occurring between E protein and the PDZ2 of ZO1 is known, the molecular details of such interactions are not completely understood. In this paper we investigate the binding reaction occurring between peptides mimicking the C-terminal region of the Envelope proteins from SARS-CoV (sequence NSSEGVPDLLV), SARS-CoV-2 (sequence NSSRVPDLLV) and MERS-CoV (sequence SKPPLPPDEWV) and the PDZ2 domain of ZO1 from kinetic and thermodynamic perspectives. The analysis of stopped-flow binding kinetic data demonstrates the ability of PDZ2 to bind the Envelope proteins from MERS-CoV with much higher kinetic parameters (microscopic association and dissociation rate constants) compared to SARS-CoV and SARS-CoV-2. Moreover, a comparison of thermodynamic equilibrium and kinetic data obtained at different ionic strength conditions is provided, highlighting dissimilar contribution of electrostatic charges in the early recognition event and in the late complex stabilization event for the three peptides. Data are discussed under the light of available structural data of PDZ2 domain of ZO1 and of previous works about these protein systems.

Results and discussion

Binding kinetics between PDZ2 and E peptides. To spectroscopically monitor the kinetics of the binding between PDZ2 of ZO1 and peptides mimicking Envelope protein we resorted to measure them through Fluorescence Resonance Energy Transfer (FRET), following an approach successfully used in the past[19]. We engineered a pseudo wild-type variant of PDZ2, by mutating the F residue in position 207–W (F207W) to act as a donor group, the acceptor being a dansyl group covalently linked to the N terminus of the peptides. Kinetic binding experiments were performed with a SX-18 Stopped-Flow apparatus (Applied Photophysics) by rapidly mixing a constant concentration of peptide mimicking the E proteins versus increasing concentrations of PDZ2 Y207W. The buffer used was Hepes 50 mM pH 7.0, and the temperature was set to 10 °C. Samples were excited at 280 nm and fluorescence emission was collected by using a 475 nm cut-off filter. For each experiment performed, 3–5 individual traces were acquired and then averaged. An increase in FRET signal could be monitored upon binding. All the averages collected were satisfactorily fitted with Eq. (1)

$$y = Aexp(-k_{obs} \cdot t) + cost \tag{1}$$

to calculate the observed rate constant of the reaction (k_{obs}).

To obtain quantitative kinetic information about the binding mechanism of PDZ2 with the three different peptides we analyzed the dependences of the calculated k_{obs} as a function of the concentration of PDZ2 (reported in Fig. 1). Data were fitted with Eq. (2)

$$k_{obs} = k_{on}[PDZ2] + k_{off} \tag{2}$$

which allows to calculate the microscopic association rate constant (k_{on}) as the slope of the straight line. Linear analysis of k_{obs} under pseudo-first order conditions would allow to extrapolate the microscopic dissociation rate constants (k_{off}) as the intercept to the y-axis. Although this procedure is correct in theory, the high experimental error that usually arises could jeopardizes a reliable calculation of k_{off}. Thus, to directly determine k_{off} values we resorted to perform displacement experiments, in which a pre-incubated complex of dansylated E peptides (at final concentration of 4 μM) and PDZ2 (at final concentration of 20 μM) were rapidly mixed with different concentrations, in high excess, of non-dansylated E peptides (ranging from 50 to 100 μM). In agreement with theory[22] the observed rate constants were found insensitive to the displacer concentrations. The displacement traces obtained for the three E peptides are reported in Fig. 1 (bottom panel). The k_{on} and k_{off} values obtained are reported in Table 1, together with the equilibrium dissociation rate constant K_D, calculated as k_{off}/k_{on}.

Data reported in Fig. 1 and Table 1 highlight the ability of the Envelope protein from MERS-CoV to reach a more rapid equilibrium with the PDZ2 of ZO1 compared to the SARS-CoV and SARS-CoV-2 Envelope proteins, and a higher affinity for PDZ2 by a factor of ~ 2. It is worth noticing, however, that the measured affinities (K_D) are all in the μM range. These values are in agreement to what is typically observed in SLiMs interactions, usually characterized by a medium–low affinity in the range of 1–500 μM[23].

The analysis of kinetic data put in evidence that, while SARS-CoV and SARS-CoV-2 E peptides show very similar binding kinetics, MERS-CoV E peptide reports a dramatically higher microscopic association and dissociation rate constants. In particular, the k_{on} measured for MERS-CoV E peptide ($10.7 \pm 0.3\ \mu M^{-1}\ s^{-1}$) is one order of magnitude higher compared to the k_{on} of SARS-CoV ($1.9 \pm 0.2\ \mu M^{-1}\ s^{-1}$) and two orders of magnitude higher compared to the k_{on} of SARS-CoV-2 ($0.6 \pm 0.1\ \mu M^{-1}\ s^{-1}$). These results may be explained by the formation of more favorable electrostatic attraction occurring in MERS-CoV E peptide than what happens for SARS-CoV

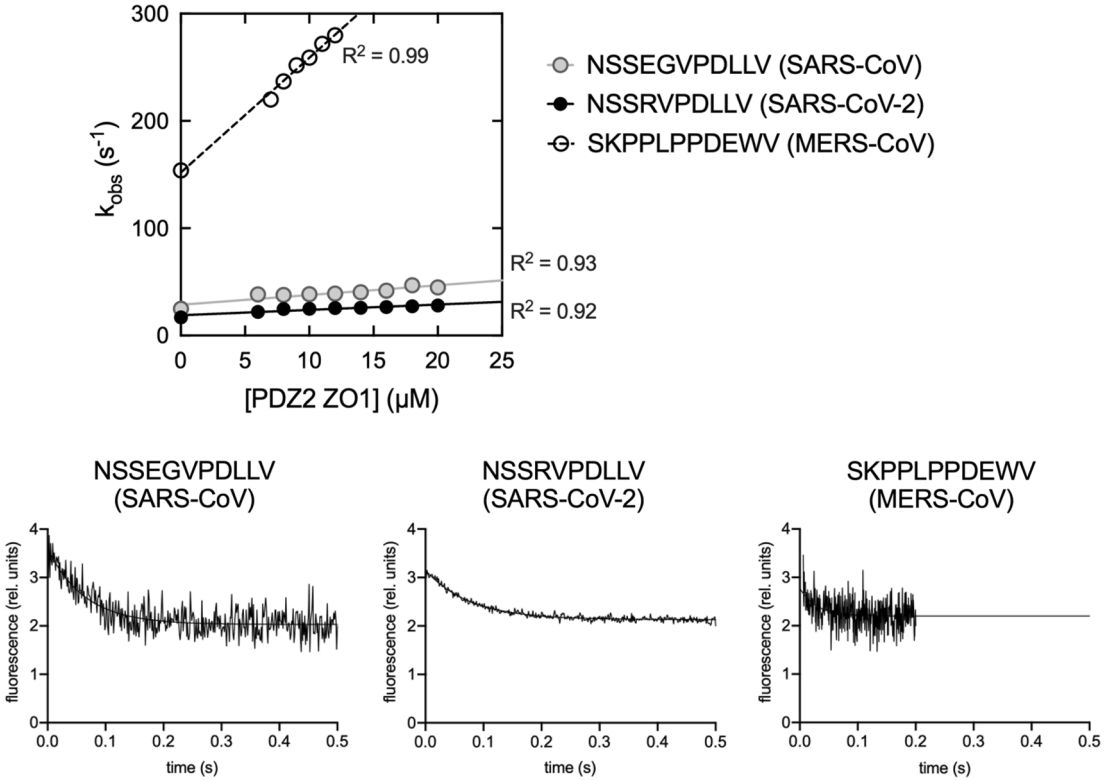

Figure 1. Top—kinetics of the binding reaction between peptides mimicking the C-terminal region of the Envelope proteins from SARS-CoV, SARS-CoV-2 and MERS-CoV versus different concentrations of PDZ2 domain of ZO1. Straight lines are the best fit to a linear equation. R^2 values for linear regression are reported. Bottom—as described in the text, points at 0 concentration of ligand were measured in separated displacement experiments. Lines are the best fit to a single exponential equation.

[NaCl]	k_{on} (μM^{-1} s^{-1})	k_{off} (s^{-1})	K_D (μM)
SARS-CoV E peptide			
0 M	1.9 ± 0.2	9.0 ± 0.1	4.7 ± 0.2
0.030 M	1.4 ± 0.2	7.0 ± 0.1	5.0 ± 0.2
0.075 M	0.8 ± 0.2	6.9 ± 0.1	8.6 ± 0.3
0.150 M	0.6 ± 0.1	6.2 ± 0.1	10.3 ± 0.2
SARS-CoV-2 E peptide			
0 M	0.6 ± 0.1	9.1 ± 0.2	15.2 ± 0.3
0.030 M	0.6 ± 0.1	9.5 ± 0.1	15.8 ± 0.2
0.075 M	0.5 ± 0.1	8.7 ± 0.2	17.4 ± 0.1
0.150 M	0.4 ± 0.1	6.8 ± 0.1	17.0 ± 0.2
MERS-CoV E peptide			
0 M	10.7 ± 0.3	154 ± 3	14 ± 1
0.030 M	*	*	19 ± 3
0.075 M	*	*	34 ± 4
0.150 M	*	*	29 ± 3

Table 1. Kinetic and affinity parameters obtained from linear fitting of data reported in Fig. 1 (top panel) and Fig. 2. Equilibrium dissociation rate constants K_D were calculated as k_{off}/k_{on} or from equilibrium binding experiments.

and SARS-CoV-2[24,25]. PDZ domains are known to recognize mainly the C-terminal carboxylate group by a "carboxylate-binding loop" conserved in the PDZ domain family[26], with the last five residues, conventionally numbered from 0, the C-terminal, to − 4, tuning their binding specificity and affinity. Typically, position 0 and − 2 are the most important in that sense, with a hydrophobic residue at position 0 required to fit into a hydrophobic pocket of PDZ domains, and a polar residue often found at position − 2 of the ligand[27]. The presence

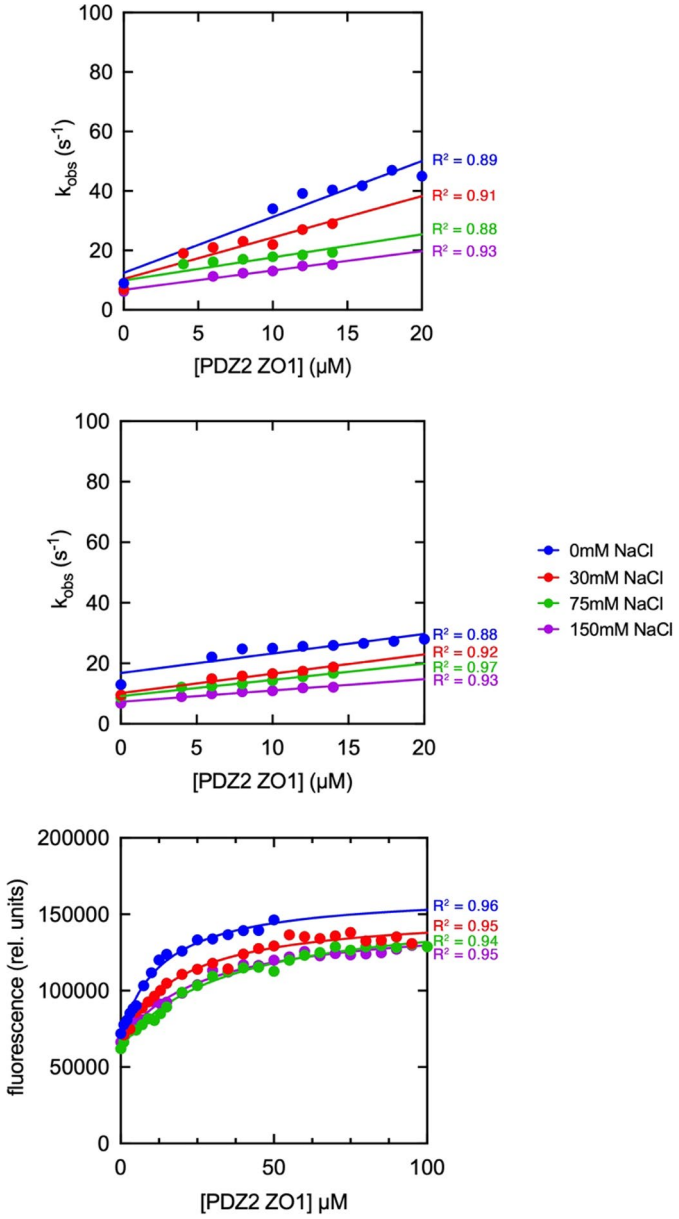

Figure 2. Ionic strength dependence of the binding reaction between SARS-CoV, SARS-CoV-2 and MERS-CoV E peptides versus different concentrations of PDZ2 domain of ZO1. Top and center panel represent stopped-flow kinetic experiments, while bottom panel represents equilibrium binding experiments at different concentrations of NaCl added to the experimental buffer. Lines are the best fit to a linear (left and center panels) and hyperbolic (right panel) equations. R^2 values are reported for all the fitting processes.

of a glutamate residue in position − 2 in the MERS-CoV E protein may be causative of the faster association reported in Fig. 1 compared to SARS-CoV and SARS-CoV-2 E proteins, that present a hydrophobic leucine in the same positions.

Ionic strength dependence of the binding reaction. To further investigate the mechanism of interaction between PDZ2 and the E peptides we resorted to monitor the binding kinetics at different experimental conditions, changing the ionic strength of the solution. Experiments were performed in buffer Hepes 50 mM pH 7.0 and progressively adding increasing concentration of NaCl (ranging from 30 to 150 mM). While for the peptide mimicking MERS-CoV E protein the addition of NaCl to the buffer caused a dramatic decrease of the amplitude of kinetic traces, such that we could not obtain any reliable kinetic data, the observed rate constants for the binding of SARS-CoV and SARS-CoV-2 E peptides at different NaCl concentrations could be measured (Fig. 2). Points at 0 μM [PDZ2] correspond to the k_{off} and were obtained by displacement experiments and data were satisfactorily fitted with Eq. (2). To measure the effect of NaCl concentration on the affinity of PDZ2 for

MERS-CoV E peptide we performed equilibrium binding experiments by keeping the E peptide at constant concentration (1 μM) and following the change of FRET signal at increasing [PDZ2]. Data obtained at 500 nm wavelength were then plotted and fitted with a hyperbolic function which returned the binding K_D.

The dependence of the logarithm of calculated K_D as function of the concentration of NaCl concentration added to the buffer are shown in Fig. 3, and their values are reported in Table 1. Increasing the ionic strength of the solution decreased the affinity of PDZ2 for the SARS-CoV and MERS-CoV E peptides, while the affinity for SARS-CoV-2 E peptide appears mostly unaffected. Moreover, a deeper analysis of kinetic data highlights that the decrease in affinity for SARS-CoV E peptide is due to a stronger effect on k_{on}. It is of interest to notice that the dependence of the log k_{on} as function of log K_D for SARS-CoV E peptide can be satisfactorily fitted with a linear equation that reported a $R^2 = 0.98$, while such correlation is absent in the case of SARS-CoV-2 peptide ($R^2 = 0.19$). These data must be interpreted comparing the sequences of SARS-CoV and SARS-CoV-2 E peptides which possess identical PDZ binding motifs (highlighted in red in Fig. 3). Thus, under the light of PDZ binding properties that have been previously discussed (and reviewed here[27]), the early events of the binding of the C-terminal portion of the E protein by the PDZ2 domain of ZO1 may be regulated by transient electrostatic interactions occurring outside of the canonical PDZ binding pocket, which then stabilizes the final docking of the protein complex. Notably, a computational analysis of the binding mechanism of the PDZ domain from protein tyrosine phosphatase 1E (PTP1E) highlighted the formation of non-native electrostatic interactions in the early events of binding that were not present in the final bound complex[28]. Our results let us hypothesize that the formation of non-native contacts in the encounter complex might be a shared characteristic of different PDZ domains.

Structural information about the PDZ2 domain of ZO1 in complex with a peptide mimicking the physiological ligand Connexin-43 (Cx43–GJA1) are available (PDB: 3CYY). An analysis of the structure of the PDZ2:Cx43 complex highlights the formation of a salt bridge between the residue K209 of the PDZ domain and the D in position − 3 of the ligand (Fig. 4). Interestingly, this residue appears to be conserved in all the three PBMs of the Envelope proteins from SARS-CoV, SARS-CoV-2 and MERS-CoV, suggesting an evolutive pressure on the gene encoding for the Envelope protein of Coronaviruses to display a SLiM able to bind the PDZ2 domain of ZO1 and hijack its physiological functions.

Another interesting point is that Cx43 possesses a hydrophobic residue (L) at − 2 position, analogously to SARS-CoV and SARS-CoV-2 E proteins. This leucine is at the interface with a positively charged residue (K246) of PDZ2 that might generate a second salt bridge with the E residue at position − 2 of MERS-CoV E protein, possibly explaining the faster association observed in kinetic binding experiments. Moreover, K246 appears to form an intramolecular salt bridge with E250 residue that may be influenced by the presence of NaCl. However, increasing the ionic strength did not affect the thermodynamic stability of PDZ2 domain (see Supplementary Materials).

Regarding the functional aspects of the formation of a second salt bridge, we can only speculate. As we mentioned in the Introduction, a common strategy for pathogens is to develop the ability to bind intracellular proteins to hijack physiological and molecular pathways in the cell. So that, when a protein can interact with more than one partner with similar affinities, protein concentrations and kinetics are fundamental in determining complex formations. Regarding the E protein, its interactions with PDZ containing proteins involved in Tight Junctions (TJs) formation is well documented[11,18–20]. Our laboratory recently published an ultrafast kinetic

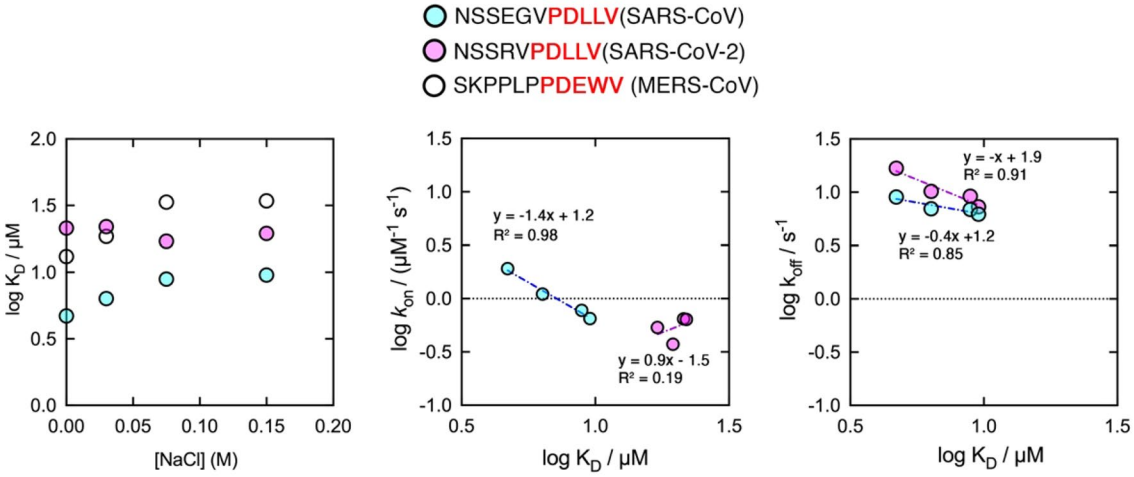

Figure 3. Left panel—dependence of equilibrium dissociation rate constant (K_D) as function of NaCl concentration added to the experimental buffer. Data show that the stability of the complex formed by SARS-CoV-2 E peptide appears to be mostly insensitive to increasing ionic strengths, while an increasing K_D is appreciable for SARS-CoV and MERS-CoV peptides at increasing [NaCl]. Center and right panel—dependence of microscopic association (k_{on}) and dissociation (k_{off}) rate constants as function of K_D. Lines represent the best fit to a linear equation. R^2 values are reported. For both SARS-CoV and SARS-CoV-2 E peptides k_{off} dependences are well described by a linear regression. On the other hand, only the k_{on} dependence of SARS-CoV peptide is well fitted by a linear equation.

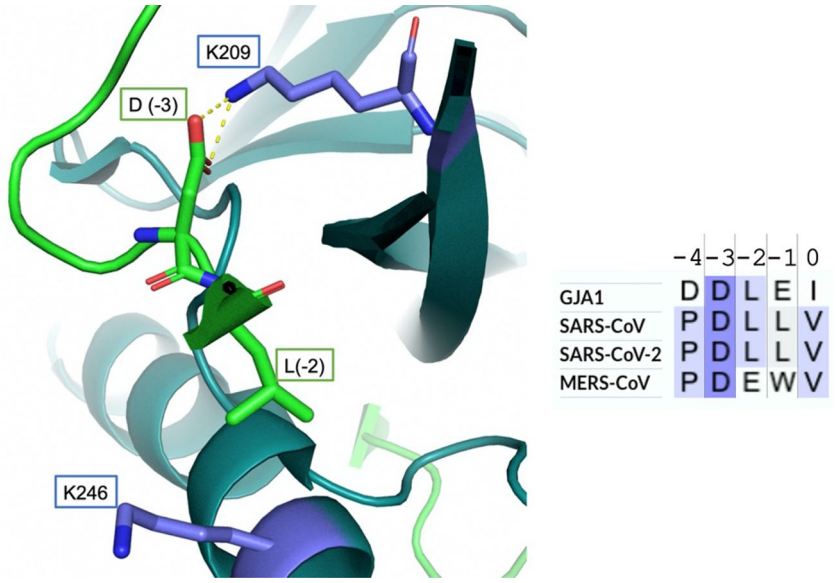

Figure 4. Structural analysis of the binding complex between the PDZ2 domain of ZO1 and a peptide mimicking the physiological ligand Connexin-43 (Cx43-GJA1) (PDB: 3CYY) and sequence alignment with SARS-CoV, SARS-CoV-2 and MERS-CoV E proteins PBMs. An electrostatic interaction between the − 3 position of the ligand and the K209 residue is highlighted as yellow dashed lines. The − 2 position of the ligand and K246 residue of PDZ2 are also highlighted. The presence of a glutamate residue in the − 2 position of the MERS-CoV E peptide may be causative of the formation of a second salt bridge, which may explain the faster association kinetics observed in the binding experiments.

analysis of the same peptides used in this work (mimicking SARS-CoV and SARS-CoV-2). Data reported much higher kinetic parameters in the binding with the PDZ domain of PALS1[19] (another protein with an important role in the formation of cellular tight junction) but with lower affinities, compared to the PDZ2 domain of ZO1. While the role of PALS1 and ZO1 in TJs formation is established, their exact molecular function is not completely understood. PDZ domains and SH3 domain of ZO1 allows it to bind several different partners and mediate the formation of TJs supramolecular complexes[29], however knock-out mice of ZO1 can form perfectly functional TJs, although with a delay in junction assembly[30]. In the case of MERS-CoV Envelope protein, our data show that the complex formation is characterized by a rapid equilibrium, that can prevent ZO1 to interact with its physiological partners possibly provoking a more effective disruption of the interactions in which ZO1 is involved, without completely compromising the TJs formation. Extensive site-directed mutagenesis, as well as a structural characterization of the PDZ2 domain in complex with Coronavirus Envelope proteins are strongly demanded in order to confirm our hypothesis, pinpoint PDZ residues directly involved in the recognition of viral peptides, and finally to pave the way towards the development of pharmaceutical strategies aimed to block this important interaction for the replication of Coronaviruses.

Conclusions

The ability of Coronaviruses Envelope protein to interact with different PDZ domain containing proteins[17–19] is a known key feature for viruses development in the intracellular environment. In this work, we show that electrostatic forces drive the binding of the Envelope proteins from SARS-CoV, SARS-CoV-2 and MERS-CoV with the second PDZ domain of ZO1. Although there are no structural data about these protein complexes, by analyzing the structure of PDZ2 domain with a physiological ligand and by comparing the sequences of the C-terminal portion of the three Envelope proteins, we propose an explanation for the highly different binding kinetics observed. In particular, the formation of salt bridges appears to be at the basis of faster association observed for MERS-CoV E peptide compared to SARS-CoV and SARS-CoV-2. Interestingly, the different effect of salt concentration on the binding of SARS-CoV and SARS-CoV-2 E peptides suggests the formation of different transient electrostatic interactions that may occur outside of the PDZ domain binding pocket. Altogether, our data and the conclusion gathered represent a step forward in the understanding of the mechanism of interaction of Coronaviruses Envelope protein with the PDZ2 domain of ZO1 and for future structural analysis aimed to characterize such complexes.

Materials and methods

Protein expression and purification. The construct encoding the PDZ2 domain of ZO1 protein was subcloned in a pET28b+ plasmid vector and then transformed in Escherichia coli cells BL21 (DE3). Bacterial cells were grown in LB medium, containing 30 µg/mL of kanamycin, at 37 °C until OD_{600} = 0.7–0.8, and then protein expression was induced with 0.5 mM IPTG. After induction, cells were grown at 25 °C overnight and then collected by centrifugation. The pellet was resuspended in buffer 50 mM TrisHCl, 300 mM NaCl,

Imidazole 10 mM, pH 8.0, adding one antiprotease tablet (Complete EDTA-free, Roche). After sonication and centrifugation, the soluble fraction from bacterial lysate was loaded onto a Ni-charged HisTrap Chelating HP (GE Healthcare) column equilibrated with 50 mM TrisHCl, 300 mM NaCl, Imidazole 10 mM, pH 8.0. Eluition was obtained by using an ÄKTA-prime system, with a gradient of Imidazole from 0 to 1 M. Fractions were analyzed through SDS-PAGE. Fractions containing the protein were collected and the buffer was exchanged to 50 mM Hepes, 150 mM NaCl, pH 7.0 by using a HiTrap Desalting column (GE Healthcare). The purity of the protein was analyzed through SDS-page. Peptides mimicking the C-terminal region of the Envelope protein from SARS-CoV, SARS-CoV-2 and MERS-CoV, with and without the dansyl N-terminal modification, were purchased from GenScript.

Equilibrium binding experiments. Equilibrium binding experiments were carried out on a Fluoromax single photon counting spectrofluorometer (Jobin-Yvon, NJ, USA), by mixing a constant concentration of dansylated MERS-CoV E peptide with increasing concetrations of PDZ2 F207W. Experiments were performed at 10 °C, using a quartz cuvette with a path length of 1 cm, in 50 mM Hepes pH 7.0 (with the addition of 0.030 M, 0.075 M and 0.15 M NaCl) measuring the change in FRET signal. The excitation wavelength was 280 nm and fluorescence spectra were recorded between 450 and 550 nm.

Stopped-flow binding and displacement experiments. Kinetic binding experiments were performed on an Applied Photophysics SX-18 stopped-flow apparatus (Applied Photophysics). Pseudo-first order binding experiments were performed mixing a constant concentration (2 μM) of dansyl-E peptide with increasing [PDZ2]. Samples were excited at 280 nm, and the emission fluorescence was recorded by using a 475 nm cutoff filter. Experiments were performed at 10 °C in buffer Hepes 50 mM pH 7.0.

As detailed in the text, microscopic dissociation rate constants were measured by performing displacement experiments. A preincubated complex of PDZ2 domain (at final concentration of 4 μM) and PDZ2 (at final concentration of 20 μM) were rapidly mixed with different concentrations, in high excess, of non-dansylated E peptides (ranging from 50 to 100 μM). Samples were excited at 280 nm and fluorescence emission was collected by using a 475 nm cutoff filter.

Data availability

The datasets generated during and/or analyzed during the current study are available from the corresponding author on reasonable request.

Received: 9 January 2023; Accepted: 12 May 2023
Published online: 16 May 2023

References

1. Hagai, T., Azia, A., Babu, M. M. & Andino, R. Use of host-like peptide motifs in viral proteins is a prevalent strategy in host–virus interactions. *Cell Rep.* **7**, 1729–1739 (2014).
2. Gouw, M. *et al.* The eukaryotic linear motif resource—2018 update. *Nucleic Acids Res.* **46**, D428–D434 (2018).
3. Mandala, V. S. *et al.* Structure and drug binding of the SARS-CoV-2 envelope protein transmembrane domain in lipid bilayers. *Nat. Struct. Mol. Biol.* **27**, 1202–1208 (2020).
4. Thiel, V. *et al.* Mechanisms and enzymes involved in SARS coronavirus genome expression. *J. Gen. Virol.* **84**, 2305–2315 (2003).
5. Torres, J. *et al.* Model of a putative pore: The pentameric alpha-helical bundle of SARS coronavirus E protein in lipid bilayers. *Biophys. J.* **91**, 938–947 (2006).
6. Gutiérrez-González, L. H. & Santos-Mendoza, T. Viral targeting of PDZ polarity proteins in the immune system as a potential evasion mechanism. *FASEB J.* **33**, 10607–10617 (2019).
7. Barreda, D. *et al.* PDZ proteins are expressed and regulated in antigen-presenting cells and are targets of influenza A virus. *J. Leukoc. Biol.* **103**, 731–738 (2018).
8. Schoeman, D. & Fielding, B. C. Coronavirus envelope protein: Current knowledge. *Virol. J.* **16**, 69 (2019).
9. Castaño-Rodriguez, C. *et al.* Role of severe acute respiratory syndrome coronavirus viroporins E, 3a, and 8a in replication and pathogenesis. *MBio* **9**, 25 (2018).
10. Jimenez-Guardeño, J. M. *et al.* Identification of the mechanisms causing reversion to virulence in an attenuated SARS-CoV for the design of a genetically stable vaccine. *PLoS Pathog.* **11**, e1005215 (2015).
11. Caillet-Saguy, C. *et al.* Host PDZ-containing proteins targeted by SARS-CoV-2. *FEBS J.* https://doi.org/10.1111/febs.15881 (2021).
12. Balda, M. S. & Matter, K. The tight junction protein ZO-1 and an interacting transcription factor regulate ErbB-2 expression. *EMBO J.* **19**, 2024–2033 (2000).
13. Sourisseau, T. *et al.* Regulation of PCNA and cyclin D1 expression and epithelial morphogenesis by the ZO-1-regulated transcription factor ZONAB/DbpA. *Mol. Cell Biol.* **26**, 2387–2398 (2006).
14. Fanning, A. S., Jameson, B. J., Jesaitis, L. A. & Anderson, J. M. The tight junction protein ZO-1 establishes a link between the transmembrane protein occludin and the actin cytoskeleton. *J. Biol. Chem.* **273**, 29745–29753 (1998).
15. Tsapara, A., Matter, K. & Balda, M. S. The heat-shock protein Apg-2 binds to the tight junction protein ZO-1 and regulates transcriptional activity of ZONAB. *Mol. Biol. Cell* **17**, 1322–1330 (2006).
16. Schmidt, A. *et al.* Occludin binds to the SH3-hinge-GuK unit of zonula occludens protein 1: Potential mechanism of tight junction regulation. *Cell Mol. Life Sci.* **61**, 1354–1365 (2004).
17. Zhu, Y. *et al.* Interactions of severe acute respiratory syndrome coronavirus 2 protein E with cell junctions and polarity PSD-95/Dlg/ZO-1-containing proteins. *Front. Microbiol.* **13**, 829094 (2022).
18. Lo Cascio, E. *et al.* Structural determinants driving the binding process between PDZ domain of wild type human PALS1 protein and SLiM sequences of SARS-CoV E proteins. *Comput. Struct. Biotechnol. J.* **19**, 1838–1847 (2021).
19. Toto, A. *et al.* Comparing the binding properties of peptides mimicking the Envelope protein of SARS-CoV and SARS-CoV-2 to the PDZ domain of the tight junction-associated PALS1 protein. *Protein Sci.* **29**, 2038–2042 (2020).
20. Chai, J. *et al.* Structural basis for SARS-CoV-2 envelope protein recognition of human cell junction protein PALS1. *Nat. Commun.* **12**, 3433 (2021).
21. Antonini, E. & Brunori, M. Hemoglobin and myoglobin in their reactions with ligands. *Science* **178**, 296 (1972).
22. Antonini, E. & Brunori, M. *Hemoglobin and Myoglobin in Their Reactions with Ligands* (North-Holland, 1971).

23. Ivarsson, Y. & Jemth, P. Affinity and specificity of motif-based protein–protein interactions. *Curr. Opin. Struct. Biol.* **54**, 26–33 (2019).
24. Schreiber, G. & Fersht, A. R. Rapid, electrostatically assisted association of proteins. *Nat. Struct. Biol.* **3**, 427–431 (1996).
25. Sheinerman, F. B., Norel, R. & Honig, B. Electrostatic aspects of protein-protein interactions. *Curr. Opin. Struct. Biol.* **10**, 153–159 (2000).
26. Harris, B. Z., Hillier, B. J. & Lim, W. A. Energetic determinants of internal motif recognition by PDZ domains. *Biochemistry* **40**, 5921–5930 (2001).
27. Nardella, C. *et al.* Targeting PDZ domains as potential treatment for viral infections, neurodegeneration and cancer. *Biol. Direct.* **16**, 15 (2021).
28. Blöchliger, N., Xu, M. & Caflisch, A. Peptide binding to a PDZ domain by electrostatic steering via nonnative salt bridges. *Biophys. J.* **108**, 2362–2370 (2015).
29. Buckley, C. E. & St Johnston, D. Apical-basal polarity and the control of epithelial form and function. *Nat. Rev. Mol. Cell Biol.* **23**, 559–577 (2022).
30. Umeda, K. *et al.* Establishment and characterization of cultured epithelial cells lacking expression of ZO-1. *J. Biol. Chem.* **279**, 44785–44794 (2004).

Acknowledgements

Work supported by the Istituto Pasteur Italia-Fondazione Cenci Bolognetti (Teresa Ariaudo Research Project 2018, Research Program 2022-2023 Under 45 Call 2020, to A.T.) and by Sapienza University of Rome (RM12218148DA1933 to A.T.).

Author contributions

Investigation, V.P., A.T.; methodology, V.P., A.T.; formal analysis, V.P., A.T.; conceptualization A.T.; writing—original draft preparation A.T.; writing—review and editing, V.P., A.T.; funding acquisition, A.T.

Competing interests

The authors declare no competing interests.

Additional information

Supplementary Information The online version contains supplementary material available at https://doi.org/10.1038/s41598-023-35079-7.

Correspondence and requests for materials should be addressed to A.T.

Reprints and permissions information is available at www.nature.com/reprints.

Publisher's note Springer Nature remains neutral with regard to jurisdictional claims in published maps and institutional affiliations.